Journal Name

ARTICLE

Secondary amine-functionalised metal-organic frameworks: direct syntheses versus tandem post-synthetic modifications

Received 00th January 20xx,
Accepted 00th January 20xx

DOI: 10.1039/x0xx00000x

www.rsc.org/

Luke L. Keenan,[a] Harina Amer Hamzah,[a] Mary F. Mahon,*[a] Mark R. Warren[b] and Andrew D. Burrows*[a]

$[Zn_4O(bdc\text{-}NH_2)_3]$, IRMOF-3 (bdc-$NH_2$ = 2-amino-1,4-benzenedicarboxylate), and $[Cr_3O(H_2O)_2F(bdc\text{-}NH_2)_3]$, MIL-101(Cr)-$NH_2$, undergo tandem post-synthetic modification reactions with aldehydes and $NaCNBH_3$ to form secondary amine-functionalised metal-organic frameworks (MOFs). The degree of conversion ranges from 17-74% for IRMOF-3 (**2a-i**) and from 35-51% for MIL-101(Cr)-NH_2 (**4a-d**), and alkene, sulfide, ferrocenyl and pyridyl substituents can be successfully introduced into the zinc MOFs. For both the zinc and chromium MOFs, an increase in the steric bulk of the aldehyde leads to a reduction in the degree of conversion. Low conversion with bulky aldehydes can be exploited to generate products containing two different secondary amine substituents, such as $[Zn_4O(bdc\text{-}NH_2)_{1.94}(bdc\text{-}NHCH_2CH_2CH_2SMe)_{0.47}(bdc\text{-}NHEt)_{0.59}]$ **2k** in which sequential tandem modifications have taken place. N_2 adsorption experiments reveal that the post-synthetically modified MOFs display lower than anticipated BET surface areas together with hysteresis. This is consistent with some degradation of crystallinity occuring on treatment with $NaCNBH_3$, as verified by control experiments, which leads to the formation of mesopores. Reactions of $H_2bdc\text{-}NH_2$ with aldehydes and $NaCNBH_3$ afforded a series of secondary amine functionalised dicarboxylic acids $H_2\mathbf{L^{1\text{-}8}}$ after acid work up. These acids were reacted with $Zn(NO_3)_2{\cdot}6H_2O$ to form the secondary amine-functionalised MOFs **5a-h** through direct synthesis. ^{1}H NMR analysis of **5a-g** showed the presence of some bdc-NH_2 linkers in addition to the secondary amine-containing linkers, and indeed the presence of $H_2bdc\text{-}NH_2$ was required for the reaction with $H_2bdc\text{-}NHCH_2Fc$ (Fc = ferrocenyl) to form a crystalline MOF. In the case of the zinc MOFs, N_2 adsorption experiments generally showed greater BET surface areas for the products of the direct synthesis reactions than for those from post-synthetic modifications suggesting that, in this case, the former is the best approach to these functionalised MOFs. In contrast, post-synthetic modification is the optimal approach to form crystalline derivatives of MIL-101(Cr)-NH_2 as direct synthesis gave amorphous products.

Introduction

Metal-organic frameworks (MOFs) have structures consisting of extended co-ordination networks of metal centres connected by bridging organic ligands.[1] There has been a rapid growth in the study of MOFs in recent years[2] due largely to their potential for porosity and the extensive range of applications that derive from this, including gas storage,[3] separations[4] and drug delivery.[5]

One advantage that MOFs possess over other porous materials is the ability to readily change the nature of their pores through functionalisation. With respect to dicarboxylate-based MOFs, dicarboxylic acids that contain an additional functionality can be employed directly in the synthesis in some cases, yielding MOFs that are isoreticular with their unfunctionalised parents.[6] Such MOFs are attractive targets, as the functionalised pore surfaces allow for greater selectivity in applications involving guest inclusion and catalysis. Many functional groups, however, cannot be incorporated directly into MOFs, as they are incompatible with the synthetic conditions. For these cases, post-synthetic modification (PSM) has emerged as a powerful tool.[7, 8] PSM involves carrying out a reaction on a pre-formed MOF, converting it into a different MOF. PSM reactions can include modifications of the secondary building unit,[9-11] metal[12-15] or ligand[16-18] exchange, or covalent transformations on the ligands. This latter class of reactions has attracted the most attention, and many such reactions have been effected on MOFs, including conversions of primary amines to amides,[19] ureas,[20] imines,[21-22] azides[23] and diazonium salts.[24] In addition, conversions of azides to triazoles,[25] aldehydes to alcohols[26] and hydrazones,[27] nitro groups to amines,[28] sulfides to sulfones,[29] and halides to

[a] Department of Chemistry, University of Bath, Claverton Down, Bath BA2 7AY,UK; e-mail: a.d.burrows@bath.ac.uk; tel: +44 (0)1225 386529.
[b] Diamond Light Source, Harwell Science and Innovation Centre, Didcot, Oxon OX11 0DE, UK.

† Electronic Supplementary Information (ESI) available: Synthetic and general experimental details, crystal structures (CCDC-1482580-1482584). See DOI: 10.1039/x0xx00000x

nitriles[30] have all been documented, as have methylations,[31] activations of aryl CH groups,[32] thermolysis reactions[33,34] and photolysis reactions.[35,36]

The conversion of a primary amine group ($-NH_2$) to an imine (–N=CHR) is a potentially attractive post-synthetic modification, as this reaction provides a simple way of introducing a wide range of R groups into the framework. This approach, however, is limited by the fact that the imine group is very susceptible to hydrolysis and reversion to the primary amine. We reported recently that reduction of the imine to a secondary amine provided a way of 'fixing' the R group into place, so a tandem modification could be employed to convert a primary amine into a secondary amine.[37] In this paper we further develop this strategy, and assess its effectiveness by comparison to the 'pre-synthetic' modification approach of reacting a metal salt with a functionalised dicarboxylic acid in a direct MOF synthesis.

Results and Discussion

Formation of secondary amine-functionalised MOFs by tandem post-synthetic modification

A range of primary amine functionalised MOFs containing 2-amino-1,4-benzenedicarboxylate (bdc-NH_2) were screened for the post-synthetic conversion of the NH_2 group into a secondary amine. Of these, studies using $[Zn_4O(bdc\text{-}NH_2)_3]$ (IRMOF-3),[6] and $[Cr_3O(H_2O)_2F(bdc\text{-}NH_2)_3]$ (MIL-101(Cr)-NH_2),[24] showed initial promise. In contrast, no significant conversion was witnessed using $[Zn_2(bdc\text{-}NH_2)_2(dabco)]$ (DMOF-1-NH_2),[38] [In(OH)(bdc-NH_2)] (MIL-68(In)-NH_2),[23] or $[Al_3O(H_2O)_2F(bdc\text{-}NH_2)_3]$ (MIL-101(Al)-NH_2).[39] In the cases of DMOF-1-NH_2 and MIL-68(In)-NH_2, PXRD confirmed that the MOF structure was retained on addition of the reagents, so the low conversion is likely to relate to poor access to the pores and/or incorrect alignment of the amine group.

IRMOF-3 was synthesised using a modification of the route reported by Cohen *et al*[19] and washed with solvent (THF) every 24 h for 3 days. MIL-101(Cr)-NH_2 was prepared by our previously reported method.[24] Our initial PSM study[37] had identified the best conditions for the tandem post-synthetic modification of the primary amine group on IRMOF-3 into a secondary amine *via* the imine using RCHO (R = Me, Et, Pr and *n*-C_7H_{15}). These reactions are summarised in Scheme 1 (**1,2a-d**).

The conversions were uniformly higher in THF than in either DMF or methanol and, furthermore, methanol led to a reduction in the product crystallinity. The products from the reactions in THF or DMF were shown by ^{11}B NMR spectroscopy to contain cyanoborohydride by-products within the pores. This was found to be preventable by the addition of a small quantity of methanol to the reaction mixture. In particular, a 15:1 THF:MeOH mixture was found to successfully remove the by-products without visually degrading the crystals. This solvent ratio had the additional benefit of preventing

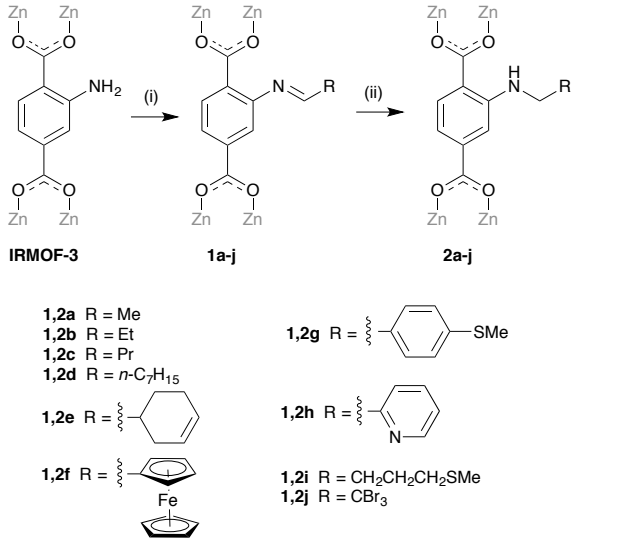

Scheme 1. PSM procedure for the conversion of IRMOF-3 into secondary amine-functionalised MOFs. (i) RCHO; (ii) $NaCNBH_3$.

formation of side-products that were observed when the reactions were carried out in neat THF. Sodium cyanoborohydride was found to be the best reducing agent, with alternatives either attacking the aldehyde prior to imine formation, or giving low conversion due to poor solubility.

Typically, IRMOF-3 was reacted with the aldehydes RCHO (R = Me, Et, Pr, *n*-C_7H_{15}), 1,2,3,6-tetrahydrobenzaldehyde (C_6H_9CHO), ferrocenecarboxaldehyde (FcCHO) and 4-methylthiobenzaldehyde ($MeSC_6H_4CHO$-4) in the presence of $NaCNBH_3$ in THF:MeOH (15:1) at 50 °C for 48 h without stirring. The resulting yellow-orange crystalline products **2a-g** were washed with THF:MeOH (15:1), then toluene, and stored under toluene.

The percentage conversions from these PSM reactions were calculated by digesting samples in DCl/D_2O and analysing the integrals in the ^1H NMR spectra (see below for more details). These percentage conversions, averaged in each case for two independent samples, are summarised in Table 1 together with the BET surface areas observed for the products.

Initial studies with 2-pyridinecarboxaldehyde to generate **2h** suggested that DMF-MeOH was a better solvent

Table 1. Percentage conversions and BET surface areas of the PSM products **2a-g**.

Compound	R	% conversion	S_{BET} / $m^2\ g^{-1}$
2a	Me	74	749
2b	Et	69	943
2c	Pr	65	823
2d	*n*-C_7H_{15}	47	659
2e	C_6H_9	49	1004
2f	Fc	27	612
2g	C_6H_4SMe-4	25	672
2h	C_5H_4N-2	22	–
2i	CH_2CH_2SMe	17	–
2j	CBr_3	0	–

combination than THF-MeOH. Using DMF-MeOH, optimum reaction conditions were established as 4 days at 50 °C. Using these parameters, the degree of conversion to the secondary amine was 22%, though some unidentified by-products were present in the ^{1}H NMR spectrum of the DCl-digested product in addition to D_2bdc-NH_2 and D_2bdc-$NHCH_2C_5H_4N$. The degree of conversion could be increased by leaving the reaction for a longer time at a higher temperature. For example, when the reaction was left at room temperature for 3 days, the conversion was only 13%, whereas a conversion of 44% was observed when the reaction was left at 50 °C for 7 days. However, leaving the reaction longer than 4 days led to some crystal degradation as witnessed by reduced intensities and broader lines in the PXRD patterns. Thus increased conversion to the secondary amine comes at a cost of decreased product crystallinity.

Preliminary reactions with 3-(methylthio)propionaldehyde to generate **2i** suggested that DMF was the optimum solvent, with addition of MeOH having no effect on the product distribution, and the presence of THF giving more by-products. The percentage conversion was 17%, and increasing the reaction time or the reaction temperature did not improve this. The ^{1}H NMR spectra of the digested products showed the presence of another compound, which was confirmed by ESI mass spectrometry to be the sulfoxide. This is believed to be formed from the sulfide during the acid digestion.

The reaction of IRMOF-3 with tribromoacetaldehyde and $NaCNBH_3$ in attempts to form **2j** gave rise to a colour change from colourless to orange using either DMF or THF as solvent. This colour became more pronounced when the reaction mixture was left to stand for a few days. ^{1}H NMR analysis, however, indicated that no conversion had occurred, with D_2bdc-NH_2 being the only dicarboxylic acid present in the digestion mixture. This suggests that the orange colour was due to Br_2, which arises from the decomposition of tribromoacetaldehyde.

As the NHR chain length was increased from *n* = 2 (**2a**) to *n* = 8 (**2d**), the degree of conversion decreased from 74% to 47%. This is consistent with previously reported post-synthetic modification reactions involving acid anhydrides[19] and isocyanates with different chain lengths,[20] and reflects the more effective pore blocking achieved when the size of the added functional group increases. In a similar manner, addition of bulky cyclohexene (**2e**), ferrocenyl (**2f**) or aromatic (**2g,h**) groups led to relatively low conversions. The powder X-ray diffraction patterns for **2a**-**i** (see ESI) confirmed that the IRMOF framework remains unaltered during the tandem PSM reactions.

The ^{1}H NMR spectra of the digested alkylamine products **2a-d** (Figures S2, S4, S6 and S8) clearly showed the presence of the expected alkyl groups. The degrees of conversion for **2a**, **2c** and **2d** were calculated by comparing the integrals of aromatic signals for D_2bdc-NH_2 and D_2bdc-NHR in the DCl-digested MOFs. D_2bdc-NH_2 arises mainly from unmodified bdc-NH_2 linkers. It is possible that some also results from hydrolysed bdc-N=CR linkers generated from reaction with the aldehyde, though overlapping peaks in the IR spectra prevented observation of any C=N stretches in **1a-d** and no aldehyde peaks could be observed in the ^{1}H NMR spectra. For **2b**, overlapping signals in the aromatic region meant it was more accurate to compare the ratio of the D_2bdc-NH_2 aromatic doublet at δ 7.64 ppm with the propyl 'sextet' at δ 3.24 ppm. The calculated conversions given in Table 1 give the formulae for **2a-d** as $[Zn_4O(bdc\text{-}NH_2)_{0.78}(bdc\text{-}NHEt)_{2.22}]$, $[Zn_4O(bdc\text{-}NH_2)_{0.93}(bdc\text{-}NHPr)_{2.07}]$, $[Zn_4O(bdc\text{-}NH_2)_{1.05}(bdc\text{-}NHBu)_{1.95}]$ and $[Zn_4O(bdc\text{-}NH_2)_{1.59}(bdc\text{-}NHC_8H_{17})_{1.41}]$, respectively. In all cases, the negative ion ESI mass spectra of the digested MOF confirmed the presence of $[Hbdc\text{-}NHR]^-$, ruling out the possibility of the alkyl groups in the NMR spectra being due to doubly *N*-alkylated linkers.

The percentage conversions for **2e-i** were calculated in a similar manner to **2a** from the integrals of the aromatic protons in the ^{1}H NMR spectra (Figures S10, S12, S14, S18, S20), giving the formulae of the modified MOFs as $[Zn_4O(bdc\text{-}NH_2)_{1.53}(bdc\text{-}NHCH_2C_6H_9)_{1.47}]$ **2e**, $[Zn_4O(bdc\text{-}NH_2)_{2.19}(bdc\text{-}NHCH_2Fc)_{0.81}]$ **2f**, $[Zn_4O(bdc\text{-}NH_2)_{2.25}(bdc\text{-}NHCH_2C_6H_4SMe)_{0.75}]$ **2g**, $[Zn_4O(bdc\text{-}NH_2)_{2.34}(bdc\text{-}NHCH_2C_5H_4N)_{0.66}]$ **2h** and $[Zn_4O(bdc\text{-}NH_2)_{2.49}(bdc\text{-}NHCH_2CH_2CH_2SMe)_{0.51}]$ **2i**. In contrast to the other members of the series, no peak for $[Hbdc\text{-}NHCH_2Fc]^-$ was observed in the negative ion ESI mass spectrum of **2f**. However, the Zn:Fe ratio observed by atomic absorption spectroscopy indicated a 23% conversion, in good agreement with the NMR results.

Single crystals of IRMOF-3 that were post-synthetically modified by ethanal were obtained and analysed by X-ray crystallography, using a synchrotron X-ray source. The data supported a formulation of $[Zn_4O(bdc\text{-}NH_2)_{1.2}(bdc\text{-}NHEt)_{1.8}]\cdot 7C_6H_5Me$ (**2a'**, 60% conversion). The overall framework topology did not change significantly during the reaction from that for IRMOF-3, in agreement with the PXRD data. Very high crystallographic symmetry, coupled with disorder and incomplete conversion, meant that only the nitrogen atom from the pendant group on the ligand could be located with any certainty. ^{1}H NMR analysis of crystals from the same batch as that used in the crystallographic study was therefore used to estimate the degree of conversion.

Thermogravimetric analyses (TGA) of **2a**-**g** (Figures S23-24), showed that, in all cases, there was an initial mass loss between 40°C and 150°C, corresponding to the loss of toluene from the samples. This was used to estimate the number of solvent molecules in the pores per formula unit as 7 for **2a**, 5.5 for **2b** and **2c**, 4 for **2d** and **2g**, 3.5 for **2e** and 2.5 for **2f**. Generally, the amount of toluene incorporated into the pores decreases with the increasing steric demand of the secondary amine substituent, which is consistent with the anticipated pore space available. The MOFs start to decompose between 270°C and 320°C and, on heating to 600°C give ZnO as the only crystalline product, as confirmed by PXRD (Figure S25).

The TGA data provided an insight into the activation conditions required for **2a-g**, and the MOFs were activated by heating at 150°C for 3 hours under reduced pressure. Nitrogen sorption isotherms for **2a-g** are shown in Figure 1, together with that for IRMOF-3, activated in a similar manner.

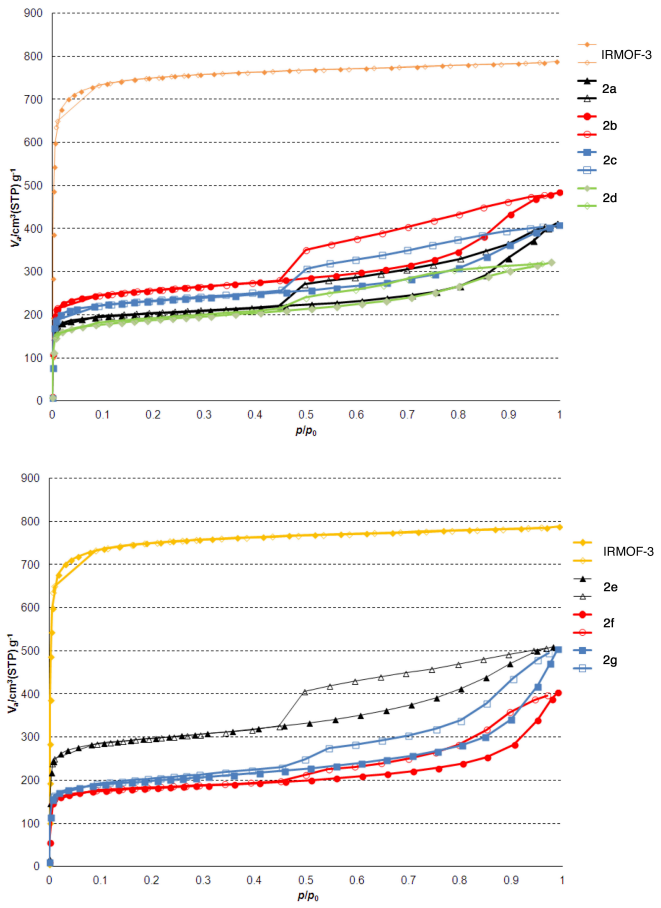

Figure 1. N_2 adsorption (filled points) and desorption (open points) curves of IRMOF-3 and **2a**-**g** at 77 K.

The lower BET surface areas (maximum S_{BET} 1004 $m^2 g^{-1}$ for **2e**) and absolute N_2 adsorptions, compared to IRMOF-3 (S_{BET} 2613 $m^2 g^{-1}$) may be partly rationalised by considering the additional mass of the secondary amino tag groups, but this mass difference is not enough to account for the total decrease in surface area observed. Notably, hysteresis is observed in the nitrogen adsorption/desorption curves of **2a**-**g**, with this being greatest for the smaller substituents. While one reason for this could be the presence of non-uniformity in tag group modification, another cause is identified from theBarrett-Joyner-Halenda (BJH) pore diameter plots (Figure S26- 27), which show the presence of mesopores that exhibit hysteresis by capillary condensation.[40] These mesopores are caused by the $NaCNBH_3$ reagent, as verified by a control experiment. IRMOF-3 treated with $NaCNBH_3$ in THF:MeOH (15:1) in the absence of an aldehyde demonstrated a reduced BET surface area of 1351 $m^2 g^{-1}$ while also displaying the same type of hysteresis as seen for **2a-g**. Washing IRMOF-3 with methanol only, gave material that did not display hysteresis in the N_2 adsorption curves, but had increased surface area (S_{BET} = 2886 $m^2 g^{-1}$) compared with IRMOF-3 treated only with toluene (S_{BET} = 2613 $m^2 g^{-1}$), perhaps due to more highly efficient washing conditions. Therefore, it is likely that crystal degradation with the hydride source in methanol is responsible for the lower than expected BET surface areas observed for **2a-g**.

As the conversion of the NH_2 group to the $NHCH_2CH_2CH_2SMe$ group (**2i**) was relatively low, it was decided to investigate whether the unmodified amino groups present in this MOF were still able to undergo modification.[41] To assess this, a sample of **2i** with the approximate formula $[Zn_4O(bdc\text{-}NH_2)_{2.5}(bdc\text{-}NHCH_2CH_2CH_2SMe)_{0.5}]$ was further reacted with propanal and $NaCNBH_3$ in a 'double tandem' process (Scheme 2) to give **2k**. After leaving the reaction mixture at room temperature for 3 days, the PXRD pattern showed no significant change (Figure S21). However, the ^1H NMR spectrum of the digested product showed the presence of a new set of peaks corresponding to D_2bdc-NHPr, with the ratio of bdc-NH_2:bdc- $NHCH_2CH_2CH_2SMe$:bdc-NHPr estimated at 65:15:20. This corresponds to an overall formula of $[Zn_4O(bdc\text{-}NH_2)_{1.94}(bdc\text{-}NHCH_2CH_2CH_2SMe)_{0.47}(bdc\text{-}NHPr)_{0.59}]$ and confirms the premise that the amino groups in **2i** remain accessible to modification, with the initial conversion to the sulfide-containing secondary amine limited by steric factors.

MIL-101(Cr) is a mesoporous MOF with pores of internal diameter 29 and 34 Å, and pore windows of 12 and 15 Å,[42] and a number of functionalised isoreticular analogues are known. Given the larger pore size than IRMOF-3, PSM on MIL-101(Cr)-NH_2 might be expected to give higher degrees of conversion. MIL-101(Cr)-NH_2 was reacted with RCHO (R = Me, Et, Pr, *n*-C_7H_{15}) in MeOH, at 50°C for 1 hour, before the addition of $NaCNBH_3$. The reaction vessel was then sealed and the contents heated to 50 °C for 72 h, without stirring. The reactions proceed through imine intermediates, **3a**-**d**, ultimately forming secondary amino tagged MOF products, of the general form MIL-101(Cr)-$NHCH_2R$, **4a**-**d** (Scheme 3).

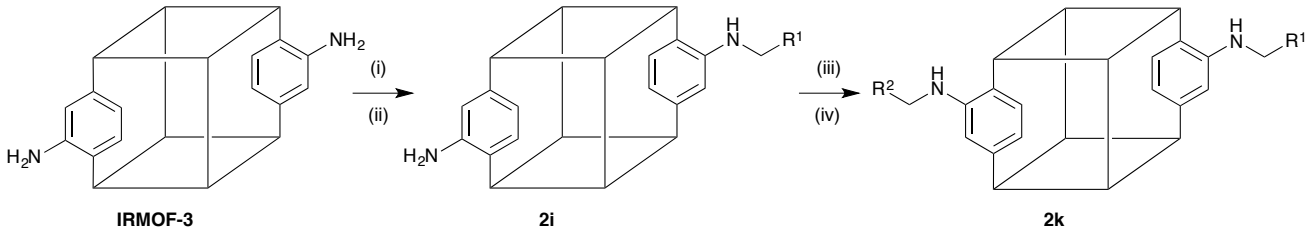

Scheme 2. The 'double tandem' PSM procedure for the conversion of IRMOF-3 into a MOF containing two secondary amine functionalities (R^1 = CH_2CH_2SMe, R^2 = Et). (i) R^1CHO, (ii) $NaCNBH_3$, (iii) R^2CHO, (iv) $NaCNBH_3$.

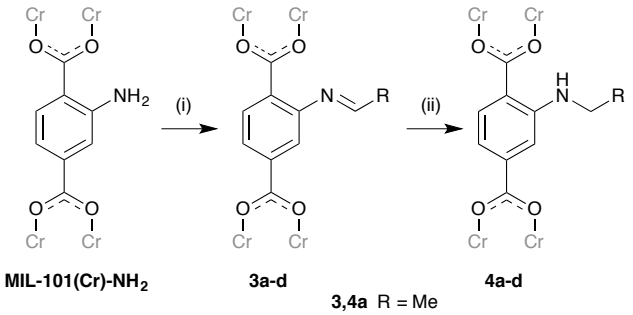

Scheme 3. Optimised PSM procedure for the conversion of MIL-101(Cr)-NH_2 into secondary amine-functionalised MOFs. (i) RCHO (4 eq.), MeOH, 50 °C, 1 h; (ii) $NaCNBH_3$ (4 eq.), MeOH, 50 °C, 72 h.

Table 2. Ligand distribution in the PSM products, **4a**-**d**, from the reaction between MIL-101(Cr)-NH_2, RCHO and $NaCNBH_3$.

Compound	R	% conversion	S_{BET} / m^2 g^{-1}
4a	Me	51	1396
4b	Et	49	1237
4c	Pr	45	1013
4d	*n*-C_7H_{15}	35	841

Percentage conversions in these tandem post-synthetic modification reactions were estimated from the ^{1}H NMR spectra of the products following digestion in NaOD/D_2O using the integrals for similar resonances to those for the IRMOF-3 studies. These results are summarised in Table 2. Under these tandem PSM reaction conditions, RCHO (R = C_6H_9, Fc and C_6H_4SMe-4) did not yield crystalline products.

The chromium MOFs show the same general trend as IRMOF-3, with the degree of conversion to the secondary amine decreasing with increasing steric bulk of the aldehyde employed. Furthermore, the conversion of NH_2 groups to secondary amines is lower for MIL-101(Cr)-NH_2 than for IRMOF-3. The PXRD patterns are broad for all samples, reflecting the small particle size (bulk material average particle size is 50 nm from SEM[24]) and the peaks become broader with increased alkyl chain length suggesting that PSM leads to some loss of crystallinity. This is supported by the BET surface area measurements, which show the same trend as for the zinc MOFs, though the reduction in the BET surface area from MIL-101(Cr)-NH_2 to **4a-d** is greater than anticipated based on that observed from IRMOF-3 to **2a-g**.

Synthesis of secondary amine-functionalised dicarboxylic acids

To investigate the synthesis of MOFs with secondary amine-functionalised linkers without using the tandem PSM reaction conditions, the dicarboxylic acids H_2bdc-$NHCH_2R$, H_2**L**$^{1-8}$, were prepared. Using the reactions summarised in Scheme 4, the secondary amine functionalised dicarboxylic acids were synthesised in 50-100% yield.

In contrast to the tandem PSM reactions carried out on IRMOF-3, the reaction of 2-aminobenzene-1,4-dicarboxylic

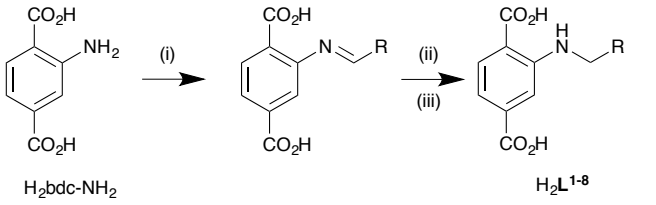

Scheme 4. Synthetic route to H_2bdc-$NHCH_2R$ (H_2**L**$^{1-8}$). R = Me (**L**^{1}), Et (**L**^{2}), Pr (**L**^{3}), *n*-C_7H_{15} (**L**^{4}), C_6H_9 (**L**^{5}), Fc (**L**^{6}), C_6H_4SMe-4 (**L**^{7}), CH_2CH_2SMe (**L**^{8}). (i) RCHO; (ii) $NaCNBH_3$; (iii) H^+, H_2O.

acid with MeCHO and $NaCNBH_3$ gave a higher isolated yield in DMF (67%) than in THF (18%) which may be due to the lower solubility of the dicarboxylic acids in THF. ^{1}H NMR analysis of the acids showed greater than 99% purity in all cases.

Attempts to isolate H_2bdc-$NHCH_2C_5H_4N$, H_2**L**^{9}, in order to prepare the pyridine-modified MOF using the pre-functionalised ligand were unsuccessful. Although it was possible to synthesise H_2**L**^{9}, it was always formed together with the borane adduct H_2bdc-$NHCH_2C_5H_4N{\cdot}BH_2CN$, which was initially identified from the ESI mass spectrum. Mittakanti and Morse have investigated the synthesis of pyridine-borane adducts as antitumor and anti-inflammatory agents.[43] They carried out a ^{11}B NMR analysis on $C_5H_5N{\cdot}BH_2CN$ and observed a signal at δ –14.7 ppm. A ^{11}B NMR spectrum on the crude product from the reaction between 2-pyridinecarboxaldehyde and $NaCNBH_3$ after acid work up showed a peak at δ –15.2 ppm which is consistent with the assigned adduct structure, as is a broad resonance in the ^{1}H NMR spectrum at δ 2.7 ppm from the BH_2 protons. All attempts to purify H_2**L**^{9} or convert H_2**L**$^9{\cdot}BH_2CN$ into H_2**L**^{9} were unsuccessful. It is notable that the borane adduct was not observed as a by-product in the PSM reaction, suggesting that the orientation of the pyridyl groups within the pores disfavours adduct formation.

Given the unsuccessful PSM reaction using tribromoacetaldehyde, it was of interest to see if the dicarboxylic acid H_2bdc-$NHCH_2CBr_3$ could be prepared from H_2bdc-NH_2, tribromoacetaldehyde and $NaCNBH_3$ to allow potential access to the MOF using the pre-functionalised linker. The reaction in methanol gave a bromine-containing product, but from a combination of ^{1}H NMR spectroscopy and ESI mass spectrometry this was identified as H_2bdc-$NHCH_2CHBr_2$. This compound could only be isolated in low quantities, so its use in MOF synthesis was not explored.

Formation of secondary amine-functionalised MOFs using prefunctionalised linkers

The reaction of $Zn(NO_3)_2{\cdot}6H_2O$ with H_2**L**$^{1-8}$ in DMF at 105°C led to the syntheses of the zinc MOFs **5a-h** as shown in Scheme 5. Unexpectedly, ^{1}H NMR analysis of the digested products showed that **5a-g** did not solely contain bdc-$NHCH_2R$ linkers, as some bdc-NH_2 linkers were also present. For the linear alkyl substituents, the proportion of bdc-NH_2 is relatively small (4-8%), though this rises to 35% for **5g** (R = C_6H_4SMe) and 80% for **5f** (R = Fc). These results are summarised in Table 3 together with BET surface areas for the products. It is currently unclear whether the bdc-NH_2 arises from preferential reaction with a

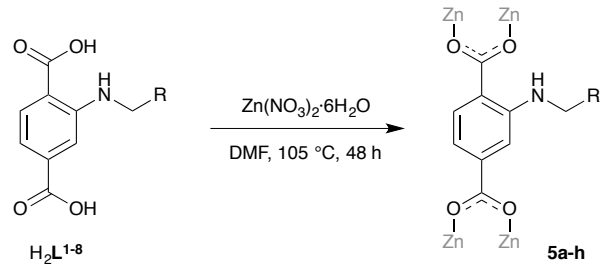

Scheme 5. Synthesis of compounds **5a-g**. R = Me (**5a**), Et (**5b**), Pr (**5c**), *n*-C_7H_{15} (**5d**), C_6H_9 (**5e**), Fc (**5f**), C_6H_4SMe-4 (**5g**), CH_2CH_2SMe (**5h**).

Table 3. IRMOF-3-NHCH$_2$R direct syntheses: percentage ligand incorporation and BET surface areas of **5a-g**.

Compound	R	% bdc-NH$_2$	% bdc-NHCH$_2$R	S_{BET} / m^2 g^{-1}
5a	Me	4	96	2238
5b	Et	7	93	1914
5c	Pr	8	92	1862
5d	*n*-C_7H_{15}	7	93	1233
5e	C_6H_9	12	88	1335
5f	Fc	80	20	1742
5g	C_6H_4SMe-4	35	65	1076
5h	CH_2CH_2SMe	0	100	871

‡ Synthesis using 88% H$_2$bdc-NHCH$_2$Fc and 12% H$_2$bdc-NH$_2$

tiny proportion of H$_2$bdc-NH$_2$ present in the dicarboxylic acids used in the synthesis or by some degradation of the secondary amines.

Although H$_2$bdc-NHCH$_2$Fc (H$_2$**L^6**) was synthesised with >99% purity, the reaction of this acid with Zn(NO$_3$)$_2$·6H$_2$O in DMF yielded only an orange-yellow non-crystalline solid. To gain access to a crystalline MOF containing this linker, H$_2$**L^6** needed to be combined with H$_2$bdc-NH$_2$ in the synthesis. Thus **5f** was prepared using a ligand mixture containing 88% H$_2$**L^6** and 12% H$_2$bdc-NH$_2$. In this case the reaction produced crystals with an average of 20% ferrocenyl incorporation, as shown by ^{1}H NMR spectroscopy of the digested MOF, demonstrating selective incorporation of bdc-NH$_2$. These results gave the molecular formula of **5f** as [Zn$_4$O(bdc-NH$_2$)$_{2.4}$(bdc-NHCH$_2$Fc)$_{0.6}$]. The exterior surfaces of the crystals were the same dark red colour as surfaces exposed on cleaving, ruling out core-shell type behaviour.[44]

The ^{1}H NMR analysis of DCl-digested **5g** revealed the presence of a third dicarboxylic acid in addition to D$_2$bdc-NHCH$_2$C$_6$H$_4$SMe and D$_2$bdc-NH$_2$. On the basis of the ^{1}H NMR analysis and the ESI mass spectrum, this compound was identified as the sulfoxide D$_2$bdc-NHCH$_2$C$_6$H$_4$S(O)Me. Analysis of the spectra over time suggested that the sulfoxide is formed during the digestion process, so the entry in Table 3 for **5g** reflects a combination of sulfide and sulfoxide. A similar observation was noted in the ^{1}H NMR spectrum of **2i** (see above).

Thermogravimetric analysis of **5a-g** (Figures S71-72) revealed similar general behaviour to the post-synthetically modified materials **2a-g**. The traces show the number of toluene

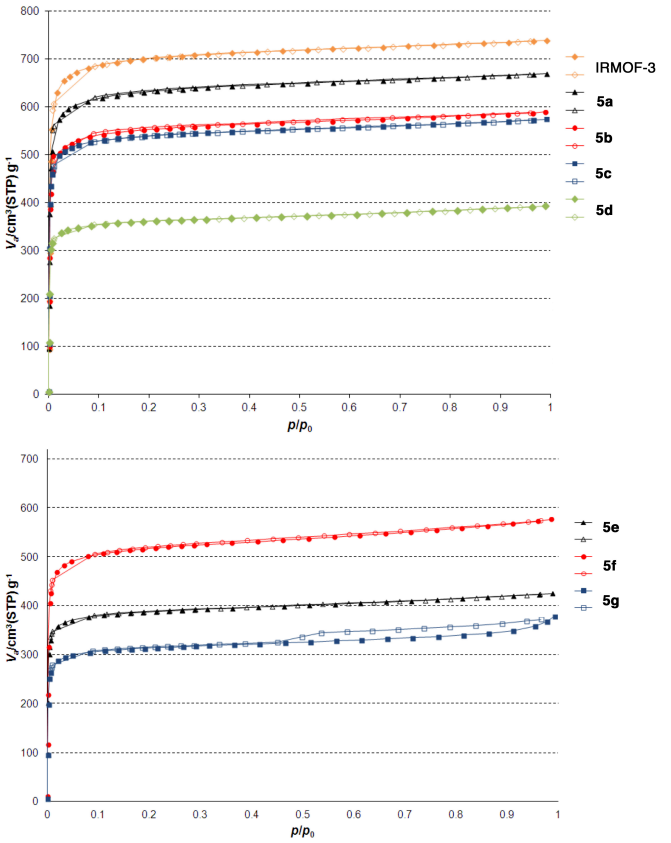

Figure 2. N$_2$ adsorption (filled points) and desorption (open points) isotherms of **5a-g** (at 77 K) and IRMOF-3.

molecules per formula unit to be 7 for **5a**, 6.3 for **5b**, 5.5 for **5c**, 4.5 for **5d**, 4.5 for **5e**, 6 for **5f** and 5.5 for **5g**.

Nitrogen adsorption isotherms for **5a-g** are shown in Figure 2. The BET surface areas are generally substantially higher than those observed for the analogous compounds **2a-g** produced by PSM. For **5a-f** the isotherms show the absence of hysteresis and the BJH plots (Figure S73-74) show no mesopores. This reflects the fact that by avoiding treating the MOFs with sodium cyanoborohydride, the degradation that leads to mesopore formation can generally be avoided. The only exception to this is **5g**, which shows some hysteresis in the isotherm and a small number of mesopores in the 20-200 nm region of the BJH plot. One reason for the larger surface area of **5f** with respect to those of **5e** and **5g** is the lower number of functionalities per pore.

The crystal structures of **5a**, **5b**, **5e** and **5g** were successfully elucidated by single crystal X-ray diffraction, using a synchrotron X-ray source. The overall framework topologies (Figure 3) match that of IRMOF-3, in agreement with the PXRD data. The cubic unit cell parameter shows a small increase with increasing length of the group within the pores (a = 25.7627(2) Å for **5a**, a = 25.8577(2) for **5e**). For all four structures the amine nitrogen atom was located and modelled with 12.5% site-occupancy, which means that the remainder of the functionalised side chains were subject to dynamic disorder

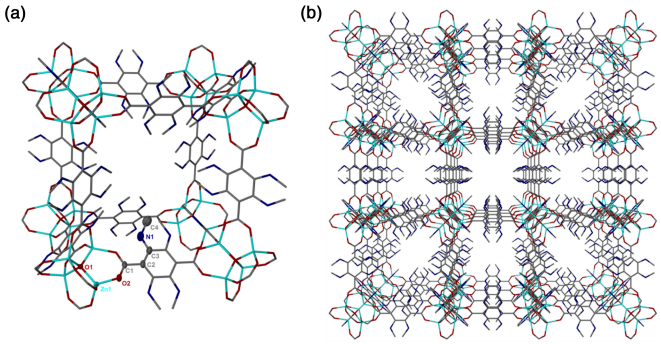

Figure 3 (a) A single pore of the pre-synthetically modified frameworks including the successfully located α-carbon (C4) of the secondary amine group in **5b** and **5e**, (b) view down the channels of the extended structure.

with the hydrogen atoms on the dicarboxylate ligand ring. For **5b** and **5e** the α-carbon atom C(4) was also located.

In contrast to the direct syntheses of **5a-h**, none of the secondary amine-functionalised dicarboxylic acids reacted with $Cr(NO_3)_3{\cdot}9H_2O$ to give analogues of MIL-101(Cr)-NH_2. Indeed, only amorphous materials were isolated from these reactions, suggesting that PSM is the only way to incorporate these secondary amine functionalities into a crystalline MOF architecture.

Experimental

Typical reactions are described here. Full experimental details are given in the ESI.

Post-synthetic modifications: Reaction of IRMOF-3 with MeCHO and $NaCNBH_3$ (2a)

IRMOF-3 (100 mg, 0.23 mmol NH_2 eq) was added to a mixture of THF:MeOH (6 mL, 15:1) in a glass vial. This was cooled in an ice bath to 5°C. Ethanal (51 µL, 0.92 mmol, 4 eq.) and then $NaCNBH_3$ (58 mg, 0.92 mmol, 4 eq.) were added to this mixture. After 30 min, the mixture was sealed and heated to 50°C for 48 h, without stirring, before cooling to ambient temperature. The crystalline product was rinsed with THF:MeOH (15:1). The resulting yellow-orange crystals were washed with toluene.

Dicarboxylic acid syntheses: 2-(Ethylamino)benzene-1,4-dicarboxylic acid, H_2bdc-NHEt (H_2L^1)

2-Aminobenzene-1,4-dicarboxylic acid (H_2bdc-NH_2) (0.200 g, 1.104 mmol) was dissolved in DMF (10 mL) and the solution was cooled to 10 °C. Ethanal (0.124 mL, 2.208 mmol) was added and the solution was stirred at 10°C for 1 h. The solution was then cooled in an ice bath and $NaCNBH_3$ (0.139 g, 2.204 mmol) was added. The resulting reaction mixture was stirred at room temperature for 24 h. The mixture was acidified with 1 M HCl, and water was added until a yellow solid precipitated. Yield: 0.146 g (63%).

Direct syntheses of functionalised MOFs: $[Zn_4O(bdc\text{-}NHEt)_3]{\cdot}7C_6H_5Me$ (5a)

H_2L^1 (46.2 mg, 0.224 mmol, 1 eq.) was dissolved in 5 mL DMF and to this was added $Zn(NO_3)_2{\cdot}6H_2O$ (200 mg, 0.672 mmol, 3 eq.). After the mixture was stirred for 30 min, the stirrer was removed, and the vessel sealed and placed in an oven at 105°C for 48 h. The resulting yellow-orange crystalline product was washed with DMF followed by toluene, then stored under toluene. Yield 28.8 mg (40%).

Conclusions

The results described in this paper demonstrate that a condensation-reduction tandem post-synthetic modification reaction can take place on IRMOF-3 and MIL-101(Cr)-NH_2, converting the primary amine group into a secondary amine functionality. The degree of conversion can be as high as 74%, though this generally decreases with increasing steric bulk of the added group. The reaction is tolerant of alkene, ferrocenyl and sulfide functionalities. In the zinc system, the addition of a small quantity of MeOH to the reaction mixture is generally necessary for removing boron containing by-products from the pores and minimising the yield of PSM by-products. This PSM process can be used to form multivariate-type MOFs, as illustrated by the formation of **2k**, which contains two different secondary amines in addition to a primary amine.

In most cases, direct syntheses of functionalised IRMOF-3-NHR frameworks were possible by reacting the modified dicarboxylic acids with $Zn(NO_3)_2{\cdot}6H_2O$. Indeed, direct synthesis of the zinc MOFs is the preferable approach, as it affords materials with higher BET surface areas than the comparable PSM analogues because damage to the frameworks by $NaCNBH_3$ is avoided. However, in the case of the ferrocenyl tag, a crystalline product was only accessible by way of a synthesis that involved using both the ferrocenyl-functionalised acid H_2L^6 and H_2bdc-NH_2 in the reaction. The resultant multivariate MOF was crystalline whereas the homoleptic MOF based on L^6 was amorphous.

In contrast to the reactions with the zinc MOFs, direct syntheses of crystalline functionalised MIL-101(Cr)-NHR frameworks was not possible. While direct synthesis may be the best way to prepare secondary amine-functionalised zinc MOFs, PSM is the only way to introduce secondary amine groups into crystalline MIL-101(Cr) MOFs.

Acknowledgements

The EPSRC and the University of Bath/Majlis Amanah Rakyat, (MARA) are thanked for studentships to LLK and HAH respectively.

Notes and references

1 H. Furukawa, K. E. Cordova, M. O'Keeffe and O. M. Yaghi, *Science*, 2013, **341**, 1230444.

2 P. Silva, S. M. F. Vilela, J. P. C. Tomé and F. A. Almeida Paz, *Chem. Soc. Rev.*, 2015, **44**, 6774.
3 M. P. Suh, H. J. Park, T. K. Prasad and D.-W. Lim, *Chem. Rev.*, 2012, **112**, 782.
4 J.-R. Li, J. Sculley and H.-C. Zhou, *Chem. Rev.*, 2012, **112**, 869.
5 P. Horcajada, R. Gref, T. Baati, P. K. Allan, G. Maurin, P. Couvreur, G. Férey, R. E. Morris and C. Serre, *Chem. Rev.*, 2012, **112**, 1232.
6 M. Eddaoudi, J. Kim, N. Rosi, D. Vodak, J. Wachter, M. O'Keeffe and O. M. Yaghi, *Science*, 2002, **295**, 469.
7 S. M. Cohen, *Chem. Rev.*, 2012, **112**, 970.
8 A. D. Burrows, in *Metal Organic Frameworks as Heterogeneous Catalysts*, eds. F. Llabrés i Xamena and J. Gascon, RSC, 2013, 31.
9 S. S.-Y. Chui, S. M.-F. Lo, J. P. H. Charmant, A. G. Orpen and I. D. Williams, *Science*, 1999, **283**, 1148.
10 M. Banerjee, S. Das, M. Yoon, H. J. Choi, M. H. Hyun, S. M. Park, G. Seo and K. Kim, *J. Am. Chem. Soc.*, 2009, **131**, 7524.
11 M. Meilikhov, K. Yusenko and R. A. Fischer, *J. Am. Chem. Soc.*, 2009, **131**, 9644.
12 T. K. Prasad, D. H. Hong and M. P. Suh, *Chem. Eur. J.*, 2010, **16**, 14043.
13 C. K. Brozek and M. Dincă, *Chem. Sci.*, 2012, **3**, 2110.
14 A. M. Shultz, O. K. Farha, D. Adhikari, A. A. Sarjeant, J. T. Hupp and S. T. Nguyen, *Inorg. Chem.*, 2011, **50**, 3174.
15 Q. Yao, J. Sun, K. Li, J. Su, M. V. Peskov and X. Zou, *Dalton Trans.*, 2012, **41**, 3953.
16 M. Kim, J. F. Cahill, Y. Su, K. A. Prather and S. M. Cohen, *Chem. Sci.*, 2012, **3**, 126.
17 O. Karagiaridi, W. Bury, A. A. Sarjeant, C. L. Stern, O. K. Farha and J. T. Hupp, *Chem. Sci.*, 2012, **3**, 3256.
18 O. Karagiaridi, M. B. Lalonde, W. Bury, A. A. Sarjeant, O. K. Farha and J. T. Hupp, *J. Am. Chem. Soc.*, 2012, **134**, 18790.
19 K. K. Tanabe, Z. Wang and S. M. Cohen, *J. Am. Chem. Soc.*, 2008, **130**, 8508.
20 E. Dugan, Z. Wang, M. Okamura, A. Medina and S. M. Cohen, *Chem. Commun.*, 2008, 3366.
21 J. A. Rood, B. C. Noll and K. W.Henderson, *Main Group Chem.*, 2009, **8**, 237.
22 M. J. Ingleson, J. Perez Barrio, J.-B. Guilbaud, Y. Z. Khimyak and M. J. Rosseinsky, *Chem. Commun.*, 2008, 2680.
23 M. Savonnet, D. Bazer-Bachi, N. Bats, J. Perez-Pellitero, E. Jeanneau, V. Lecocq, C. Pinel and D. Farrusseng, *J. Am. Chem. Soc.*, 2010, **132**, 4518.
24 D. Jiang, L. L. Keenan, A. D. Burrows and K. J. Edler, *Chem. Commun.*, 2012, **48**, 12053.
25 Y. Goto, H. Sato, S. Shinkai and K. Sada, *J. Am. Chem. Soc.*, 2008, **130**, 14354.
26 W. Morris, C. J. Doonan, H. Furukawa, R. Banerjee and O. M. Yaghi, *J. Am. Chem. Soc.*, 2008, **130**, 12626.
27 A. D. Burrows, C. G. Frost, M. F. Mahon and C. Richardson, *Angew. Chem. Int. Ed.*, 2008, **47**, 8482.
28 S. Bernt, V. Guillerm, C. Serre and N. Stock, *Chem. Commun.*, 2011, **47**, 2838.
29 A. D. Burrows, C. G. Frost, M. F. Mahon and C. Richardson, *Chem. Commun.*, 2009, 4218.
30 M. Kim, S. J. Garibay and S. M. Cohen, *Inorg. Chem.*, 2011, **50**, 729.
31 L. Xu, Y. Luo, L. Sun, S. Pu, M. Fang, R.-X. Yuan and H.-B. Du, *Dalton Trans.*, 2016, **45**, 8614.
32 W.-Y. Gao, H. Wu, K. Leng, Y. Sun and S. Ma, *Angew. Chem. Int. Ed.*, 2016, **55**, 5472.
33 R. K. Deshpande, J. L. Minnaar and S. G. Telfer, *Angew. Chem. Int. Ed.*, 2010, **49**, 4598.
34 D. J. Lun, G. I. N. Waterhouse and S. G. Telfer, *J. Am. Chem. Soc.*, 2011, **133**, 5806.
35 K. K. Tanabe, C. A. Allen and S. M. Cohen, *Angew. Chem. Int. Ed.*, 2010, **49**, 9730.
36 R. K. Deshpande, G. I. N. Waterhouse, G. B. Jameson and S. G. Telfer, *Chem. Commun.*, 2012, **48**, 1574.
37 A. D. Burrows and L. L. Keenan, *CrystEngComm*, 2012, **14**, 4112.
38 Z. Wang, K. K. Tanabe and S. M. Cohen, *Inorg. Chem.*, 2009, **48**, 296.
39 P. Serra-Crespo, E. V. Ramos-Fernandez, J. Gascon and F. Kapteijn, *Chem. Mater.*, 2011, **23**, 2565.
40 Y. Yoo and H.-K. Jeong, *Chem. Eng. J.*, 2012, **181-182**, 740.
41 Z. Wang and S. M. Cohen, *Angew. Chem. Int. Ed.*, 2008, **47**, 4699.
42 G. Férey, C. Mellot-Draznieks, C. Serre, F. Millange, J. Dutour, S. Surblé and I. Margiolaki, *Science*, 2005, **309**, 2040.
43 M. Mittakanti and K. W. Morse, *Inorg. Chem.*, 1990, **29**, 554.
44 K. Koh, A. G. Wong-Foy and A. J. Matzger, *Chem. Commun.*, 2009, 6162.